Marine and Petroleum Geology 22 (2005) 403–412

Marine and Petroleum Geology

www.elsevier.com/locate/marpetgeo

Gas hydrate occurrence on the continental slope of the northern South China Sea

S. Wu[a,*], G. Zhang[b], Y. Huang[b], J. Liang[b], H.K. Wong[c]

[a]*Institute of Oceanology, Chinese Academy of Sciences, 266071 Qingdao, China*
[b]*Guangzhou Marine Geological Survey, MLR, 510760 Guangzhou, China*
[c]*Institute of Biogeochemistry and Marine Chemistry, University of Hamburg, D-20146 Hamburg, Germany*

Received 15 July 2003; received in revised form 20 November 2004; accepted 27 November 2004

Abstract

High-resolution multi-channel seismic data and geological samples were collected during two research cruises of the R/V FENDOU 4 in 1999 and 2000. Studies on these data and samples together with results from sites 1143–1145 and 1148 of ODP Leg 184 suggest that the geological structure on the continental slope of the northern South China Sea is favorable for the formation of gas hydrates. Bottom simulating reflectors (BSRs) and geochemical anomalies which indicate the existence of gas hydrates have been recognized in sediments of the Xisha Trough, the Dongsha Rise and the accretionary wedge of the Manila subduction zone. These gas hydrates are generated by two different mechanisms depending on the tectonic regime and the seismic and geochemical characteristics. The first applies to the passive continental margin of the northern South China Sea on the Dongsha Rise and in the Xisha Trough. The gas hydrates are associated with diapiric structures, active faults, slumps and gravity flows as well as high Late Cenozoic sedimentation rates. Their seismic expression includes BSRs, seismic blanking zones and velocity anomalies. The second mechanism is operative on the active continental margin along the Manila subduction zone, especially in the accretionary wedge. Here, gas hydrate occurrence is marked by widespread BSRs and acoustic 'pull-down' possibly related to the existence of free gas in the sediments beneath the BSR. The thickness of the seismic blanking zones averages 250 m, suggesting that the stable gas hydrate zone has about the same thickness.

Keywords: Gas hydrate; Bottom simulating reflector; Geological structure; South China Sea

1. Introduction

Gas hydrate is a solid composed of water and to a large extent methane formed under low temperature and high pressure conditions (Sloan, 1998). Methane can migrate into the gas hydrate stability zone (GHSZ) along active faults or diapir structure bodies, where it is converted into gas hydrate to cement the porous sediments (Milkov and Sassen, 2003; Ginsburg and Soloviev, 1997). Gas hydrate usually forms at about 0–1100 m below the seafloor (mbsf) at water depths of 300–2000 m. The thickness of a single gas hydrate layer varies from several tens of centimeters to several meters and the area of distribution is of the order of 10^4–10^5 km^2 (Gornitz, 1994; Kvenvolden, 1998; Milkov and Sassen, 2001; Mori, 2002; Sloan, 1998).

In 1999, the Guangzhou Marine Geological Survey (GMGS), China, conducted a research cruise to explore gas hydrates in the Xisha Trough. A total of 500 line-km of high-resolution multi-channel seismic profiles were collected. Important seismic indicators for gas hydrate (Andreassen, 1995; Hyndman and Davis, 1992; Paull et al., 1996) were recognized in this area for the first time. These include bottom simulating reflectors (BSR, identified along 150 km of the cruise track), BSR polarity inversion, blanking zones (BZ), and wave velocity anomalies (Yao, 2001; Zhang et al., 2002).

Subsequently in 2000, an additional high-resolution seismic survey and geological sampling were carried out by GMGS in the Xisha Trough and on the Dongsha Rise. The extent of BSR occurrence was enlarged and

* Corresponding author. Tel.: +86 532 2898543; fax: +86 532 2898544.
E-mail address: swu@ms.qdio.ac.cn (S. Wu).

0264-8172/$ - see front matter © 2005 Elsevier Ltd. All rights reserved.
doi:10.1016/j.marpetgeo.2004.11.006

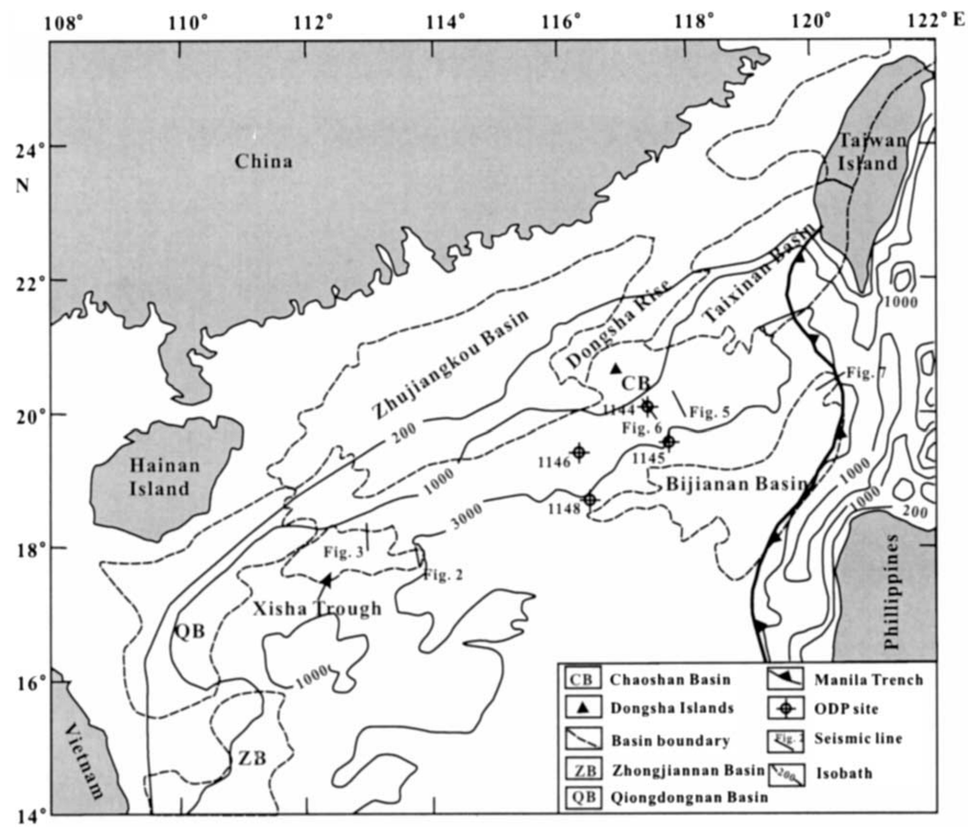

Fig. 1. Tectonic elements of the northern South China Sea. Short thick lines: the position of seismic profiles; fine lines: bathymetry; dashed lines: major tectonic boundary; solid line with triangles: subduction zone.

geochemical anomalies indicative of gas hydrates were mapped. Gas hydrate in the sediment was found to compose mainly of methane, ethane and propane (Zhu et al., 2000).

The northern South China Sea is a promising area for gas hydrate (Song and Geng, 2000; Wu et al., 2004; Zhang and Chen, 2000; Zhang et al., 2002). Tectonically, the northwestern part of our study area (including the Zhujiangkou Basin, Xisha Trough, Dongsha Rise and the Chaoshan Basin, Fig. 1) is a typical passive continental margin, while the northeastern part is an active convergent margin. Here, the South China Sea block (Eurasian Plate) collides with the Luzon Island Arc along the Manila subduction zone since 12 Ma (Teng, 1990), with the Taixinan and Bijianan basins marking the accretionary wedge (Fig. 1).

The purpose of this paper is to study the seismic and geological characteristics of gas hydrate-cemented sediments and to discuss their formation on the continental slope of the northern South China Sea using high-resolution seismic data and sediment samples obtained in recent years.

2. Seismic expressions of gas hydrates on the continental slope of the northern South China Sea

The BSRs hitherto recognized in the northern South China Sea can be subdivided into two types according to their seismic characteristics and the associated tectonic regime. The first is found on the passive continental margin of the northern South China Sea, e.g. in the Xisha Trough and on the Dongsha Rise. The second is encountered in the accretionary wedge of the Manila subduction zone and the adjacent Bijianan Basin.

2.1. Characteristics of the BSR on the continental slope of the passive margin

Xisha Trough is a Cenozoic extensional basin developed on the northwestern continental slope of the South China Sea. BSRs were recognized in the north and south of this trough (Fig. 2). Other seismic indicators for gas hydrates observed include blanking zones, velocity anomalies (Fig. 3), and waveform polarity inversions. Because of the prevalent horizontal stratification, the BSRs are generally parallel to the sediment bedding except locally. They are widespread within the water depth range of 350–3000 m, and lie 200–750 ms (about 180–750 m) bsf. Blanking zones are common above the BSR (Fig. 3). They may be a result of homogenization of the sediment and hence their elastic properties and with it a reduction in the impedance contrast across the sedimentary strata because of gas hydrate-cementation of the sediment (Hyndman and Davis, 1992; Rempel and Buffett, 1997). The thickness of the blanking

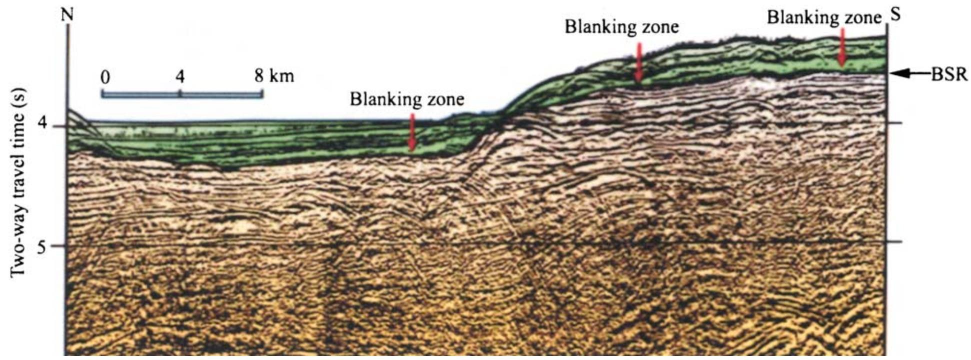

Fig. 2. Seismic profile in the Xisha Trough obtained during a Chinese–American joint project in 1985 on board the R/V HAIYANGSIHAO and CONRAD (profile no. 19), showing active faults and the BSR. See Fig. 1 for profile location.

zones varies from 80 to 620 m, averaging 350 m. This thickness, which is interpreted to correspond to the thickness of the gas hydrate-cemented layer (von Huene and Pecher, 1999; Holbrook et al., 1996), correlates positively with the measured gas hydrate content of the sediment, at least on the northern Cascadia continental slope (Yuan et al., 1996).

The seismic velocity of gas hydrate-bearing sediments is usually higher than that of sediments without gas hydrate (Shipley et al., 1979; Singh et al., 1993). It can reach 1.85–2.5 km/s (Fig. 4), and is strongly correlated with the hydrate concentration. If free gas exists beneath the BSR which marks the lower boundary of the thermobaric GHSZ, this velocity can decrease rapidly to 0.5–0.2 km/s, yielding a 3-layer velocity profile characterized by ‘top and bottom low, and middle high’. The interval velocity of the blanking zone above the BSR (interpreted as the GHSZ) increases distinctly, averaging 2612 m/s in the Xisha Trough compared to 2096 m/s below the BSR.

The Dongsha Rise is a basement high that has subsided since the onset of rifting of the South China Sea in the mid-Miocene. During this time, a large thickness of sediment accumulated at a high sedimentation rate. The tectonic structure and evolution of the Dongsha Rise are similar to that of the Blake Ridge on the eastern seaboard off North America which is rich in gas hydrates (Paull et al., 1996). Our seismic profiles show that a BSR occurs at 0.4–0.7 s (about 650 m) bsf (Fig. 5; Wang et al., 2000). The thickness of the blanking zone above the BSR is about 150 m (0.2 s) (Fig. 6).

2.2. BSRs on the northeastern active continental margin

Along the northeastern boundary of the South China Sea where the South China Sea block is subducting under Luzon, a large, thick accretional wedge formed in the eastern parts of the Taixinan and Bijianan basins (Fig. 1). Marked BSRs with accompanying polarity reversal compared to the seafloor reflector have been recognized in this accretionary wedge with synsedimentary deformations (McDonnel et al., 2000; Fig. 7). These BSRs cross-cut the bedding planes of the sediment, although identification in the western Bijianan Basin is difficult because here the stratification is almost horizontal.

The phenomenon of ‘velocity pull-down’ is observed along some of the BSRs in the accretionary wedge. The same phenomenon exists in the eastern Nankai trough, it is affected by the existence of free gas under the gas

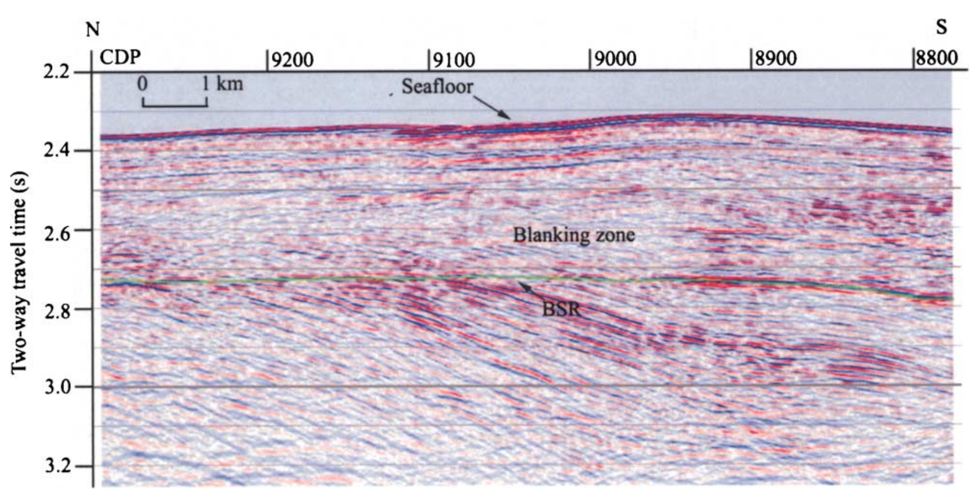

Fig. 3. Seismic profile in the Xisha Trough, showing the blanking zone above a distinct BSR. See Fig. 1 for profile location.

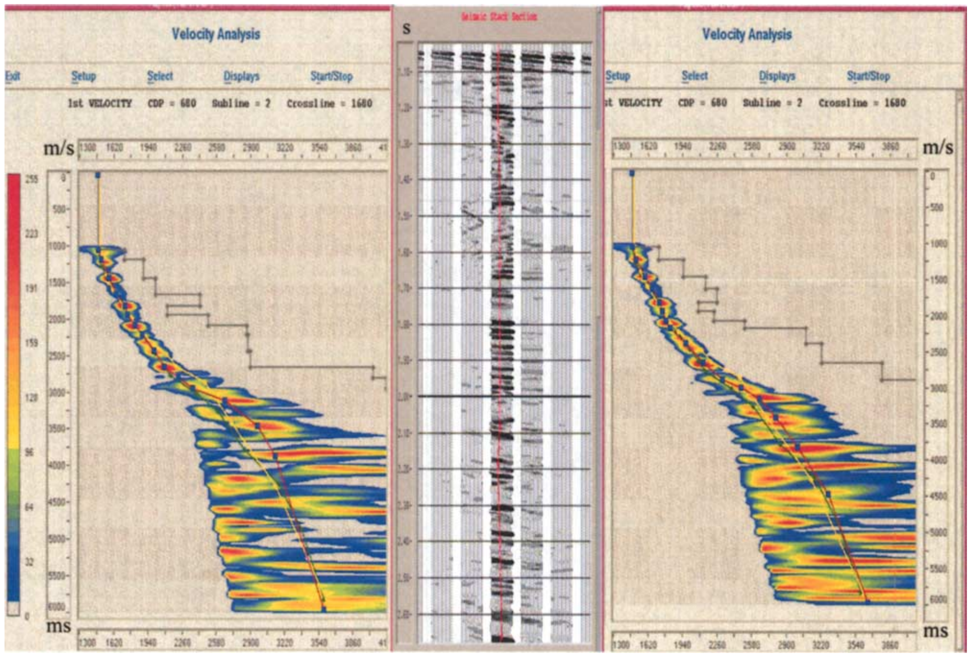

Fig. 4. Velocity sections in the Xisha Trough. (A) High interval velocity (2420 m/s), low velocity (2100 m/s); (B) high velocity (2260 m/s), low interval velocity (2100 m/s).

hydrate layer (Nouzé et al., 2004). Here, the average thickness of the blanking zone (or the GHSZ) is estimated to be around 250 m using a migration interval velocity of the gas hydrate-cemented sediments above the BSR of 2183 m/s. Our CDP gathers suggest that the BSR is quasi-parallel to the seafloor and that its amplitudes varies with migration offset.

The geothermal gradient on the northeastern active continental margin is 44 °C/km which were obtained by seafloor heat flow measurements (Yao et al., 1994), and it is higher than the geothermal gradient in adjacent areas. This reflects the heating effect of the transitional crust on the lower continental slope. The measured heat flow is comparable to those reported for accretionary wedges elsewhere (Ashi et al., 2002), and is favorable for the formation of gas hydrates as deep thermogenic gas migrates upwards into the shallow sediments.

3. Geochemical anomalies of the gas hydrate-cemented sediments

3.1. Xisha Trough

Some geochemical anomalies are indicators for the existence of gas hydrates. Here, we shall describe the anomalies we measured in the Xisha Trough using various analytical methods (including thermoluminescence) on pore water, acidolysis hydrocarbons and headspace gas.

The chloride concentration, δ^{18}O and δD are low in the pore water of shallow sediments. The chloride content varies between 19.1 and 25.8 ml^{-1} and decreases with increasing depth. This suggests that very little gas hydrate is to be expected in the shallow sediments. However, the content of free gas in the sediment rises gradually with depth (Fig. 8), while sulfate in the pore water decreases rapidly

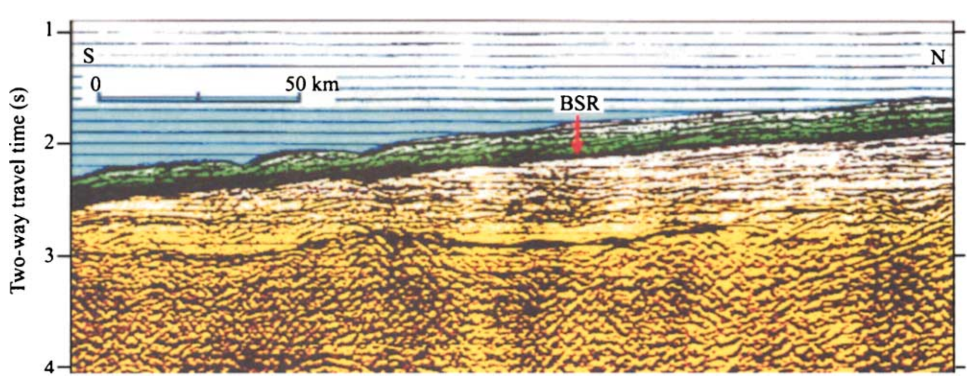

Fig. 5. Seismic profiles in the Dongsha Trough, showing active faults and the BSR. See Fig. 1 for profile location.

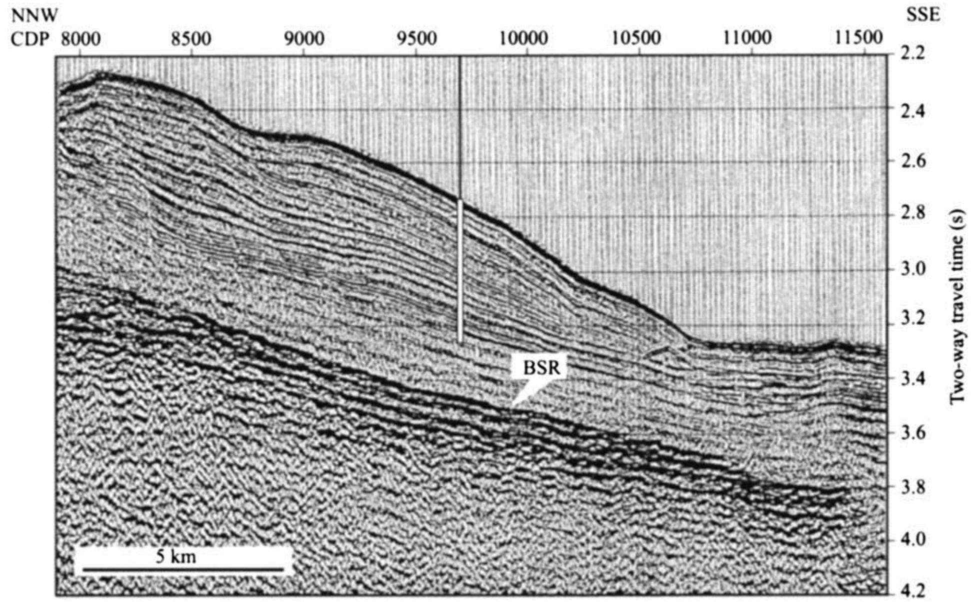

Fig. 6. Seismic profile 10 from cruise 95 of the German R/V Sonne across site 1144 of ODP Leg 184 in the northern South China Sea, showing a clear BSR and the blanking zone. See Fig. 1 for profile location.

with depth in the sediment. The sulfate reduction zone is only 25 mbsf. The values at site 1144 and site 1146 of ODP Leg 184 are 11 and 65 mbsf, respectively. At site 1146, marked anomalies in the pore water chloride concentration which indicates the presence of gas hydrate in the depth of 65–540.41 mbsf have been reported (Zhu et al., 2002). Therefore, we suggest that while gas hydrate is rare or absent in the shallow sediments of the Xisha Trough, it is present at greater sediment depths.

The existence of gas hydrates in the Xisha Trough can also be inferred from results of acidolysis hydrocarbon and thermoluminescence analyses. Thus, the organic carbon content in the sediment lies in the range of 0.15–1.39%, with relatively high contents of ethane and butane, so that the C1/(C2+C3) ratio is low (70.1). Headspace gas content in the Xisha Trough reaches 0.1–6.9 μl/kg with traces of ethane (Fig. 8). Therefore, we infer that the gas encountered is largely thermogenic. This is consistent with the δ^{13}C values of CH4 (-37.8 to -24.0‰) from ODP Leg 184, which are mostly thermogenic gas source (Wang et al., 2000; Zhu et al., 2000) (Fig. 9).

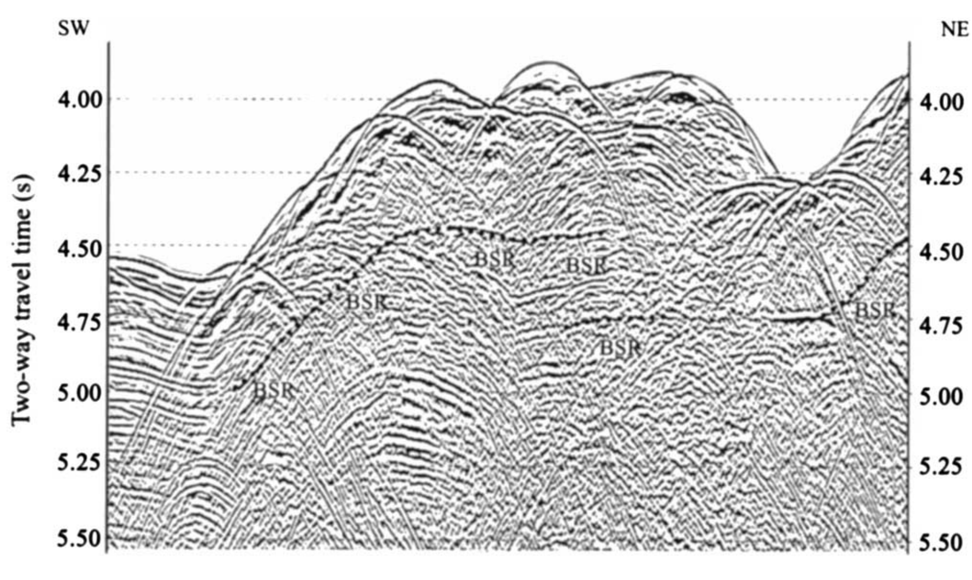

Fig. 7. Seismic profile in the accretionary wedge of the Manila subduction zone, showing two BSRs. The dotted lines indicate the BSRs. See Fig. 1 for profile location.

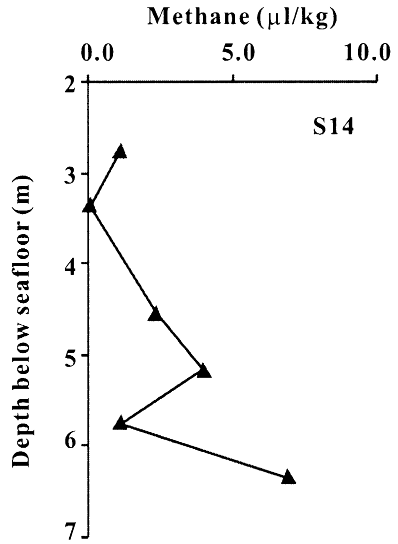

Fig. 8. Variations in methane content of headspace gas in cuttings of sediments at coring station S14 in the Xisha Trough.

3.2. Dongsha Rise

Geochemical anomalies also exists in the Dongsha area. Here, the chloride content in the pore waters ranges from 17.8 to 26.9 ml^{-1}, decreasing with depth. Headspace gas has been reported from site 1144 of ODP Leg 184. Its methane content reaches a maximum in the depth interval 300–600 mbsf. Geochemical anomalies measured at site 1146 include, in addition to headspace gas, high pore water chloride content and high concentrations of methane, ethane and propane (Zhu et al., 2002). Chloride concentration in the pore waters decreases rapidly at 540.41 mbsf. Maybe it is the depth of decomposition of gas hydrates. Assuming that the seafloor temperature is 3.14 °C and the geothermal gradient is 24 °C/km (Gong and Li, 1998), the lower boundary of the GHSZ is estimated to be at 690 mbsf. This is in general agreement with the BSR depth obtained from our seismic profiles (200–700 m).

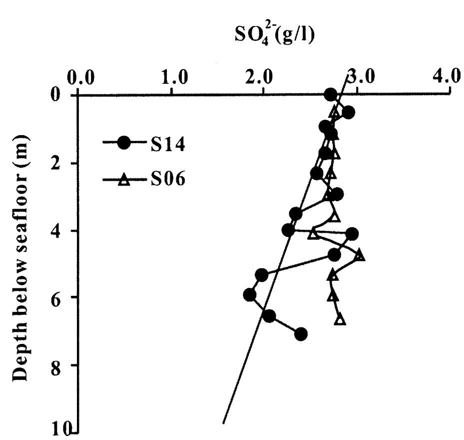

Fig. 9. Variations in sulfate content in the pore waters of cores S6 and S14 in the Xisha Trough.

4. Geological constraints on gas hydrate formation in the northern South China Sea

4.1. Tectonic constraint

The area favorable to gas hydrate formation in the northern South China Sea is about 1.4×10^6 km^2, of which 84% is on the continental slope (Zhang et al., 2002). However, a BSR is not always present on the lower slope (Wu et al., 2004). Geological factors such as sedimentary environment, tectonics, temperature and pressure conditions, rate of gas supply and reservoir conditions control the formation and distribution of gas hydrates. Among these factors, tectonics often plays an important role (Mori, 2002; Paull et al., 1996; Reed et al., 1990; Rowe and Gettrust, 1993).

The northwestern South China Sea is a passive continental margin with a 550 km wide continental slope (Feng et al., 1992; Gong and Li, 1998). Here, active NE–SW trending faults are well developed (Lüdmann et al., 2001) and mud and magma diapiric structures are widespread on the Dongsha Rise and its vicinity. Three tectonic movements, namely the Nanhai, Dongsha and Liuhua movements, took place in the early Miocene, the Pliocene, and the Pleistocene, respectively (Lüdmann et al., 2001; Feng et al., 1992). Neotectonic activities, in particular active normal faulting, submarine slide and mud diapir structures have left their imprint on the continental slope. Those faults that outcrop on the seafloor control the present-day bathymetry and act as extensive pathways for fluid flow.

On the northeastern continental slope, BSRs were recognized in the accretionary wedge of the Manila subduction zone. Similar BSR (and gas hydrate) occurrences have been reported elsewhere under a comparable geotectonic setting. Examples are: South Shetland Trench, Peru Trench, Central America Trench, Cascadia Trench, Nankai Trough, and Luzon Trench (e.g. Milkov and Sassen, 2001; von Huene and Pecher, 1999; Yuan et al., 1996; Nouzé et al., 2004). Accretionary wedges constitute a favorable geological setting for gas hydrates (von Huene and Pecher, 1999) because subduction creates favorable thermodynamic conditions.

4.2. Submarine morphology and sediment facies

The morphology of the continental slope in the northern South China Sea include troughs, seamounts, terraces, deep sea channels and submarine fans. A thick sediment section of deltaic to hemipelagic facies has been deposited since the mid-Miocene onset of rifting in the central South China Sea (Wu et al., 1999). Rifting was succeeded by a rapid regional thermal subsidence since 17 Ma. At sites 1143 and 1144 of ODP Leg 184 southeast of the Dongsha Islands, the sedimentation rates during the past million years are 0.4–1.2 and 0.15–0.21 m/ka, respectively (Wang et al., 2000). These high sedimentation rates lead to sediment overpressure, conditions that are favorable for the preservation of hydrates. Likewise, well-developed mud diapirism in the northern South China Sea facilitates the upward migration of deep thermogenic and shallow biogenic gas to accumulate as gas hydrates. Similar sedimentary conditions are found in the northern Bay of Bengal in the Indian Ocean where gas hydrates also occur (Subrahmanyam et al., 1998).

4.3. Gas source

The major Cenozoic sedimentary basins on the continental slope of the northern South China Sea are the Zhujiangkou, Chaoshan, Bijianan and Taixinan basins in addition to the Xisha Trough. These basins accumulated large thicknesses of organic-rich sediments (2–11 km) at high sedimentation rates. Analyses of the composition of light hydrocarbons in piston cores from the Xisha Trough show high concentrations of hydrogen, methane and ethane, decreasing downcore. Total organic carbon is usually more than 0.8% in the Late Cenozoic sediments. The carbon isotopic composition o methane and molecular ratio (C1/C2+C3) indicate that the hydrocarbon is thermogenic gas or mixed gas at sites 1144 and 1146 of ODP Leg 184 (Wang et al., 2000; Zhu et al., 2002). Mass wasting is common on the northwestern continental slope due to rapid deposition and active tectonics since the Late Miocene. More than 2 km of sediments deposited in the Qiongdongnan Basin during the Quaternary, which provide an abundant biogenic gas source needed for gas hydrate formation.

4.4. Temperature and pressure conditions for gas hydrate stability

The conditions for gas hydrate stability include temperatures at the sea surface and of the bottom waters, geothermal gradient, hydrostatic pressure (water depth), and lithostatic pressure. Some authors suggest that the burial depth and thickness of gas hydrates are related to bottom water temperature, geothermal gradient, and pressure (Xu and Ruppel, 1999; Zatsepina and Buffett, 1997). The lower the seafloor temperature, the thicker the GHSZ. Statistics show the seafloor temperature is about 2–6 °C (Fig. 10). Jin and Wang (2002) indicate that the gas hydrate in the northern South China Sea keep stable in sediments at water depth greater than 550 m. The gas hydrate thickness decreases with geothermal gradient, but increases with water depth.

The geothermal gradient is not uniform in the northern South China Sea and tends to increase with water depth. On the northwestern continental slope, it varies generally within the range of 32–40 °C/km, averaging 37.6 °C/km (Yao, 1994; Spanger and Hayes, 1995). Spanger and Hayes (1995) estimated using linear regression that the geothermal gradient here lies between 23.6 and 41.6 °C/km. In the Zhujiangkou Basin, it is generally 30–40 °C/km (Gong and

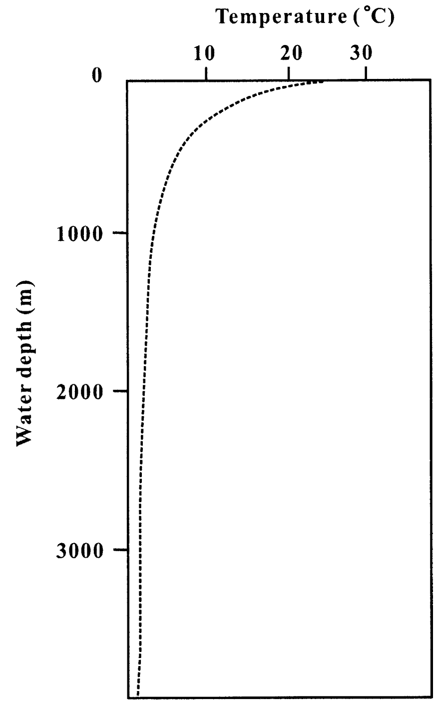

Fig. 10. Seafloor temperature as a function of water depth in the Xisha Trough.

Li, 1998; Yao, 1994). In the westernmost Xisha Trough, the average geothermal gradient reaches 40 °C/km according to seafloor heat flow measurement (Yao, 1994); this is significantly higher than the average geothermal gradient (35 °C/km) in the Zhujiangkou Basin. On the whole, the geothermal gradient increases gradually from the Zhujiangkou Basin to the Xisha Trough.

The geothermal gradients measured at two deep-water sites (site 1145, 3175 m water depth and site 1148, 3294 m) on the continental slope in the vicinity of the Dongsha Islands of ODP Leg 184 are high, viz. 83 and 90 °C/km, respectively (Wang et al., 2000). In comparison, the gradients at two shallower sites (site 1144, 2037 m; site 1146, 2092 m) are lower (24 and 59 °C/km, respectively). This difference is due to extension of the continental margin (Spanger and Hayes, 1995; Gong and Li, 1998). The deeper sites are located near the continent–ocean boundary and heat migrates upward from the high-temperature lower crust. The shallow sites are blanketed by a thick layer of sediment and tectonic activity is rare.

Heat flow distribution in the South China Sea is likewise non-uniform. In the sedimentary basins of the northern South China Sea, it generally lies in the range 60–80 mW/m^2 with an average of 74.9 mW/m^2. There is an increasing trend basinward, and this increase is a function of lithospheric thinning. Generally, locally high heat flow is associated with thermal fluid migration near fracture zones and magmatic activity near the crustal continent–ocean transition.

The water depth in the Xisha Trough is about 350–3200 m, the bottom water temperatures are 1–5 °C, averaging 3 °C. The heat flow varies from 42 to 121 mW/m^2 (Yao, 1994) and the geothermal gradient reaches 40 °C/km. Despite these high heat flow values and high geothermal gradients, gas hydrate formation in the Xisha Trough is still possible given the appropriate pressure conditions.

BSRs have been observed on seismic profiles in the Xisha Trough (Song and Geng, 2000; Yao, 2001; Zhang and Chen, 2000). Because their occurrence is P–T dependent, they provide a useful method to estimate the thermal gradient where direct measurements are unavailable (Shipley et al., 1979), or allow an independent check on the recognition of the BSR where heat flow measurements exist. BSRs have been recognized at water depths between 390 and 2540 m and burial depths of 283–734 m below the seafloor in the Xisha Trough. The thickness of the stable gas hydrate-cemented sediment layer ranges from 95 to 457 m (Table 1). From the BSR to the top of the gas hydrate layer, the prevailing temperature and pressure conditions should lie within the GHSZ.

The average bottom water temperature decreases with water depth approximately exponentially in the Xisha Trough (Fig. 10). Measurements and interpolation show that this temperature is about 3.56 °C at 1000 m water depth. For water depths exceeding 1000 m, the bottom water temperature decreases very slowly from 3.56 to about 2.57 °C. To estimate the theoretical BSR depth, we assumed an average bottom water temperature of 3 °C, and an average geothermal gradient of 40 °C/km. The computed results from 40 positions on seismic profiles where a BSR occurs are shown in Fig. 11. For all except four of these positions, the P–T conditions lie within the GHSZ. Thus, we conclude that

Table 1
BSR burial depths (lower boundary of the GHSZ) in the world (after Zhu et al., 2000; Zhang et al., 2002)

Region	Water depth (km)	BSR depth (km)
Blake Ridge	2.3–5.0	0.5–0.6
New Jersey continental slop	2.6–3.0	0.6–0.7
Gulf of Mexico	1.2–2.0	0.5–0.6
Southern Caribbean Sea	1.5–2.0	0.5
Central America: slope off Mexico	2.2–3.5	0.4–0.6
Central America: inner trench slope off Guatemala	1.5–3.0	0.5–0.6
Central America: inner trench slope off Nicaragua	1.1–2.2	0.4–0.5
Central America: inner trench slope off Costa Rica	0.8–1.5	0.5–0.6
Central America: inner trench slope off Panama	2.2–2.3	0.5–0.6
Japan Trench: inner slope	0.8–4.3	0.5–0.6
Kermadec Trench	2.0–2.6	0.5–0.6
Hawke Gulf	0.8–2.3	0.5–0.7
Gulf of Oman	2.8–3.0	0.6–0.7
Bering Sea	1.7–2.2	0.6–0.7
Xisha Trough (South China Sea)	0.39–2.54	0.28–0.73

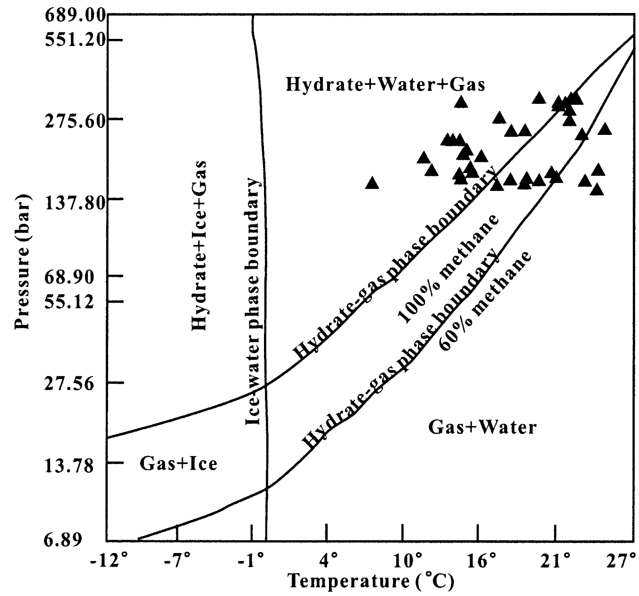

Fig. 11. Pressure and temperatures conditions for gas hydrate formation in the Xisha Trough.

gas hydrates can form at water depths greater than 320 m in the Xisha Trough, and that the thickness of the gas hydrate layer increases with the content of (C3 + C4).

5. Mechanism of gas hydrate formation and volume of gas bound in gas hydrates in the northern South China Sea

5.1. Mechanism of gas hydrate formation

Based on the analysis of gas hydrate in sediments, P–T conditions for the GHSZ, geochemical anomalies and seismic attributes especially of the BSR (Bangs et al., 1993; Paull et al., 1996), we believe that gas hydrate-cemented sediments exist on the continental slope of the northern South China Sea, in particular southwest of the Dongsha Islands, on the slope and basin floor of the Xisha Trough, and in the accretionary wedge of the Manila subduction zone (Fig. 1). BSRs continuous at least over a large distance have been imaged in our seismic profiles from the slope and trough floor of the Xisha Trough (Figs. 2 and 3), the Dongsha Rise (Figs. 5 and 6), and the accretionary wedge of the Manila subduction zone (double BSRs, Fig. 7).

There are several mechanisms of gas hydrate formation in the northern South China Sea. Gas hydrates in the Xisha Trough are dominated by biogenic gas that is abundant in this Cenozoic sedimentary basin. The biogenic gas migrates into the GHSZ along active faults or within a diapir. Southeast of the Dongsha Islands, however, large amounts of thermogenic gas form at depth and merge with the biogenic gas generated at shallower levels. The accretionary wedge of the Manila subduction zone is marked by double BSRs (Fig. 7) found also in the Nankai Trough (Ashi et al., 2002). During tectonically active periods, the thermogenic gas migrates together with the pore fluid upwards along thrusts or detached faults to the GHSZ, where the sediment becomes gas hydrate-cemented. We speculate that because tectonic activity is high, the lower boundary of the GHSZ here may be unstable, whereby gas hydrates can gasify and continue its upward migration.

5.2. Volume of gas bound in the form of gas hydrate in the northern South China Sea

To attempt an order-of-magnitude estimate of the amount of gas preserved in the form of gas hydrate at the base of the stability zone (Q), we note that (Gornitz, 1994)

$$Q = A \times \Delta z \times \phi \times H \times E \times R$$

where A is the area of BSR occurrence; Δz, average thickness of the layer of gas hydrate-cemented sediments; ϕ, average effective sediment porosity; H, hydrate-filled pore volume; E, gas expansion factor for methane; and R, degree of hydrate mineralization.

We assumed a gas hydrate occurrence on 50% of the continental slope (1.18×10^6 km^2), an average thickness of the gas hydrate zone of 350 m, a sediment porosity of 50%, and a gas hydrate saturation of 5%. The methane expansion factor is 164, and the degree of hydrate mineralization is 10%. This yields a volume of 8.5×10^{13} m^3 for the gas bound in gas hydrates in the northern South China Sea, or the equivalent of 8.5×10^{13} tons of oil. We note that this is an optimistic estimate. (1) From the literature, we know that a discussion of the choice of numerical values for the parameters involved is very important. For above parameters, BSRs were widely distributed in the northern South China Sea by the natinal gas hydrate investigation program. And blank zones are usually conplay on the seismic profiles. The blank zone is interpreted the thickness of gas hydrate in the Blake Ridge because the seismic amplitude decreases in the gas hydrate filled sediments zone (Paull et al., 1996). Area of gas hydrate occurrence (A) and thickness of the layer of gas hydrate-cemented sediments (Δz) could be determined by seismic data. Sediment porosities can be determined from analyses of recovered cores and from borehole log measurements. The average sediment porosities with gas hydrate-bearing interval in the Blake Ridge have been determined to range from about 30 to 80%, with average 50% (Paull et al., 1996). The ODP drilling wells only located in the Dongsha Rise of the northern South China Sea. The porosities vary from 30 to 60%, so we choice 50% in our calculation. The gas hydrate saturations range from 0% to maximum near 20% in the would, usually less than 10% in the Blake Ridge (Paull et al., 1996). And the saturation has difference according to measurement methods. (2) The amount of free gas trapped below the lower boundary of the GHSZ should also be estimated, although it is in general several orders of magnitude smaller.

6. Conclusions

(1) We infer from our geophysical and geochemical data that gas hydrate is widespread on the continental slope of the northern South China Sea. Single and double BSRs have been recognized on the Dongsha Rise as well as in the Xisha Trough and the accretionary wedge of the Manila subduction zone. The BSR usually occurs in 350–3000 m water depth, and is buried at 200–750 ms (180–790 m) bsf. The average thickness of the gas hydrate-cemented sediment layer is about 350 m. Geochemical anomalies that provide indirect evidence for gas hydrates include chloride and sulfate concentrations in the pore water, amount and composition of acidolysis hydrocarbon and headspace gas, and thermoluminescence. They suggest that sediments deep in the sedimentary column are richer in gas hydrates than shallow sediments.

(2) Because of high sedimentation rates, appropriate prevailing temperature and pressure conditions, abundant sources for gas, effective gas migration pathways, gas reservoirs and an active tectonic setting, conditions for gas hydrate formation are favorable on the continental slope of the northern South China Sea.

(3) The geothermal gradient lies generally in the range of 32–40 °C/km with an average of 37.6 °C/km on the continental slope of the northern South China Sea. The depth range of 390–2540 m provides temperature and pressure conditions favorable to the formation of gas hydrates in sediments of the Xisha Trough.

(4) There are several mechanism for gas hydrate formation on the continental slope of the northern South China Sea: biogenic gas generation followed by gas migration in the Xisha Trough, biogenic and thermogenic gas generation with migration southeast of the Dongsha Islands, in situ gas generation with little migration on the Dongsha Rise, and thermogenic gas generation under a compressive regime and subsequent gas migration in the accretionary wedge of the Manila subduction zone. The conditions that must be satisfied include: abundant gas source (deep thermogenic and shallow biogenic), appropriate temperature and pressure conditions, high sedimentation rates and tectonic activity. The total volume of gas bound in gas hydrates is estimated to be on the order of 1.5×10^{13} m^3.

Acknowledgements

We would like to thank the Guangzhou Marine Geological Survey for permission to publish these data. The research reported here is supported by the Knowledge Innovation Project of the Chinese Academy of Sciences (Grant No. KZCX3-SW-219) and the National Science Foundation of China (Grant No. 40276022).

References

Andreassen, K., 1995. Seismic studies of a bottom simulating reflection related to gas hydrate beneath the continental margin of the Beaufort Sea. Journal of Geophysical Research 100 (B7), 12659–12673.

Ashi, J., Tokuyama, H., Taira, A., 2002. Distribution of methane hydrate BSRs and its implication for the prism growth in the Nankai Trough. Marine Geology 187, 177–191.

Bangs, N.L., Sawyer, D.S., Golovchenko, X., 1993. Free gas at the base of the gas hydrate zone in the vicinity of the Chile triple junction. Geology 21 (10), 905–908.

Feng, Z., Miao, W., Zheng, W., Chen, S., 1992. Structure and hydrocarbon potential of the para-passive continental margin of the northern South China Sea. In: Watkins, J.S., Feng, Z., McMillen, K.J. (Eds.), Geology and geophysics of continental margins. AAPG Memoirs, 53, pp. 27–41.

Ginsburg, G.D., Soloviev, V.A., 1997. Methane migration within the submarine gas-hydrate stability zone under deep-water conditions. Marine Geology 137, 49–57.

Gong, Z.S., Li, S.T., 1998. Continental Margin Basin Analysis and Hydrocarbon Accumulation in the Northern South China Sea. Science Press, Beijing. 510 pp.

Gornitz, V., 1994. Potential distribution of methane hydrates in the world's ocean. Global Biogeochemical Cycles 8, 335–347.

Holbrook, W.S., Hoskins, H., Wood, W.T., Stephen, R.A., Lizarralde, D., et al., 1996. Methane and free gas on the Blake Ridge from vertical seismic profiling. Science 273, 1840–1843.

Hyndman, R.D., Davis, E.E., 1992. A mechanism for the formation of methane hydrate and seafloor bottom simulating reflectors by vertical fluid expulsion. Journal of Geophysical Research 97 (B5), 7025–7041.

Jin, C., Wang, J., 2002. A preliminary study of the gas hydrate stability zone in the South China Sea. Acta Geologica Sinica 76 (4), 423–428.

Kvenvolden, K.A., 1998. A primer on the geological occurrence of gas hydrate. In: Henriet, J.P., Mienert, J. (Eds.), Gas Hydrates Relevance to World Margin Stability and Climate Change. The Geological Society, London, pp. 9–30.

Lüdmann, T., Wong, H.K., Wang, P.X., 2001. Plio-quaternary sedimentation processes and neotectonics of the northern continental margin of the South China Sea. Marine Geology 172, 331–358.

McDonnel, S.L., Max, M.D., Cherkis, N.Z., Czarneeki, M.F., 2000. Tectono-sedimentary controls on the likelihood of gas hydrate occurrence near Taiwan. Marine & Petroleum Geology 17, 929–936.

Milkov, A.V., Sassen, R., 2001. Estimate of gas hydrate resource, northwestern Gulf of Mexico continental slope. Marine Geology 179, 71–83.

Milkov, A.V., Sassen, R., 2003. Preliminary assessment of resources and economic potential of individual gas hydrate accumulations in the Gulf of Mexico continental slope. Marine & Petroleum Geology 20, 111–128.

Mori, Y.H. (Ed.), 2002. Proceedings of the Fourth International Conference on Gas Hydrates, Yokohama, Japan, May 19–23, vol. 1, pp. 1–294.

Nouzé, H., Henry, P., Noble, M., Martin, V., Pascal, G., 2004. Large gas hydrate accumulations in the eastern Nankai Trough inferred from new high-resolution seismic data. Geophysical Research Letters 31, 13308–13331.

Paull, C.K., Matsumoto, R., Wallace, P.J., et al., 1996. Proceedings of the Ocean Drilling Project, Initial Reports, 164. College Station, Taxes (Ocean Drilling Program). 623 pp.

Reed, D.L., Silver, E.A., Tagudin, J.E., Shipley, T.H., Vrolijk, P., 1990. Relations between mud volcanoes, thrust deformation, slope sedimentation, and gas hydrate, offshore North Panama. Marine & Petroleum Geology 7 (1), 44–54.

Rempel, A.W., Buffett, B.A., 1997. Formation and accumulation of gas hydrate in porous media. Journal of Geophysical Research 102, 10151–10164.

Rowe, M.M., Gettrust, J.F., 1993. Faulted structure of the bottom simulating reflector on the Blake Ridge, western North Atlantic. Geology 21 (9), 833–836.

Shipley, T.H., Houston, M.H., Buffler, R.T., Shaub, F.J., McMillen, K.J., Ladd, J.W., Worzel, J.L., 1979. Seismic evidence for widespread possible gas hydrate horizon on continental slopes and rises. AAPG Bulletin 63, 2204–2213.

Singh, S.C., Minshull, T.A., Spence, G.D., 1993. Velocity structure of a gas hydrate reflector. Sciences 260, 204–207.

Sloan, E.D., 1998. Clathrate Hydrates of Natural Gases, second ed. Marcel Dekker Inc., New York, 628 pp.

Song, H.B., Geng, J.H., 2000. Geophysical evidence of gas hydrates existence in Dongsha region north of South China Sea. EOS Transactions on AGU 81 (48), 635.

Spanger, N.S., Hayes, D.E., 1995. Gravity, heat flow, and seismic constraints on the processes of crust extension: northern margin of the South China Sea. Journal of Geophysical Research 100, 22447–22483.

Subrahmanyam, C., Reddi, S.I., Thakur, N.K., Rao, T.G., Sain, K., 1998. Gas-hydrates: a synoptic view. Journal of the Geological Society of India 52 (5), 497–512.

Teng, L.S., 1990. Geotectonic evolution of Late Cenozoic arc-continental collision in Taiwan. Tectonophysics 183, 57–76.

von Huene, R., Pecher, I.A., 1999. Vertical tectonics and the origins of BSRs along the Peru margin. Earth and Planetary Sciences Letters 166, 47–55.

Wang, P., Prell, W.L., Blum, P., et al., 2000. Proceeding of the Ocean Drilling Program, Initial Reports 184, College Station, Taxes, 623 pp.

Wu, S., Wong, H.K., Lüdmann, T., 1999. Gravity-driven sedimentation on the northwestern continental slope of the South China Sea: results from high-resolution seismic data and piston cores. Chinese Journal of Oceanology and Limnology 17 (2), 155–169.

Wu, S., Zhang, G., Guo, C., Zhong, S., Huang, Y., 2004. Geological constraints for the formation and distribution of gas hydrate in the Dongsha Islands and adjacent sea area. Acta Petroleum Sinica 25 (4), 7–12.

Xu, W., Ruppel, C., 1999. Predicting the occurrence, distribution, and evolution of methane gas hydrate in porous marine sediments. Journal of Geophysical Research 104 (B3), 5081–5095.

Yao, B.C., 2001. Gas hydrates in the South China Sea. Journal of Tropical Oceanology 20 (2), 20–28.

Yao, B., Zeng, W., Hayes, D.E., Spanger, S., 1994. The Geological Memoir of South China Sea Surveyed Jointly by China & USA. China University of Geosciences Press, Wuhan, pp. 1–201.

Yuan, T., Hyndman, R.D., Spence, G.D., Desmons, B., 1996. Seismic velocity increase and deep-sea gas hydrate concentration above a bottom-simulating reflector on the northern Cascadia continental slope. Journal of Geophysical Research 101 (6), 13655–13671.

Zatsepina, O.Y., Buffett, B.A., 1997. Phase equilibrium of gas hydrate; implications for the formation of hydrate in the deep-sea floor. Geophysical Research Letters 24, 1567–1570.

Zhang, G.X., Chen, B.Y., 2000. Methane hydrate resources and prospect in the South China Sea. Haiyang Dizhi 3, 1–9.

Zhang, G.X., Huang, Y.Y., Zhu, Y.H., Wu, B.H., 2002. Prospect of gas hydrate resources in the South China Sea. Marine Geology and Quaternary Geology 22 (1), 75–81 (in Chinese).

Zhu, Y.H., Matsumoto, R., Huang, Y.Y., 2000. Gas hydrate in the South China Sea: chlorine and methane anomaly at site 1146, ODP leg 184. EOS Transactions on AGU 81 (22), WP61.

Zhu, Y.H., Huang, Y., Matsumoto, R., Wu, B., 2002. Geochemical and stable isotopic compositions of pore fluids and authigenic siderite concretions from site 1146, ODP Leg 184: implication for gas hydrate. In: Prell, W.L., Wang, P., Rea, D.K., Clemans, S.C. (Eds.), Proceedings of the ODP, Scientific Results, V184, pp. 1–15.